Search for Double Gamma-Ray Emission from the First Excited States of O^{16} and C^{12}†

D. E. ALBURGER AND P. D. PARKER
Brookhaven National Laboratory, Upton, New York
(Received 13 March 1964)

Two-dimensional pulse-height analysis has been used to search for double gamma-ray emission in competition with the $E0(\pi)$ decay of the 6.05-MeV state in O^{16} and in competition with the $E2$ gamma-ray decay of the 4.43-MeV state in C^{12}. In each case two 5-in.×5-in. NaI crystals viewed the target located at the center of a double-conical lead-Hevimet absorber, and the outputs of these detectors were connected to a 64×64 two-dimensional pulse-height analyzer. Coincidence patterns were analyzed for the presence of a line of constant sum-energy with an intensity distribution peaked at the center in accordance with the theoretical $E^3(E_0-E)^3$ distribution. In neither case was any evidence obtained for such a pattern. Upper limits of $\Gamma_{E1E1}/\Gamma_{E0(\pi)}\leq 1.1\times 10^{-4}$ for the 6.05-MeV state of O^{16} and of $\Gamma_{E1E1}/\Gamma_{E2}\leq 0.5\times 10^{-4}$ for the 4.43-MeV state C^{12} were derived.

INTRODUCTION

A NUMBER of experiments have been carried out in search of double gamma-ray emission in nuclear transitions. One search has been made for double gamma-ray emission from the 4.43-MeV 2^+ first excited state in C^{12} which normally decays by an $E2$ gamma-ray transition. McCallum, Bromley, and Kuehner[1] measured coincident gamma rays at several resonances in the $N^{15}(p,\alpha)C^{12}$ reaction using two NaI detectors and a modified Hoogenboom circuit for analysis of the events. An upper limit of $\Gamma_{E1E1}/\Gamma_{E2}\leq 1.7\times 10^{-4}$ was set for the decay of the 4.43-MeV state of C^{12}. Double gamma-ray emission has also been searched for in competition with the isomeric $M4$ decay of the 12-day 163.9-keV state of Xe^{131}. Alväger and Ryde[2] interpreted their data for this decay as showing positive evidence for double gamma emission in this case; however, the existence of an intermediate level at an excitation of 80.2 keV[3,4] in Xe^{131} casts some doubt on their interpretation.

In most instances, however, decay by the emission of two gamma rays has been looked for in competition with electric monopole transitions. Three such cases that have been studied are the first excited states of O^{16}, Ca^{40}, and Zr^{90}. A positive effect of $N_{\gamma\gamma}/N\approx 2.3\times 10^{-3}$ was reported by Langhoff and Hennies[5] for the 1.75-MeV transition in Zr^{90}. However, this result has not been confirmed either by Ryde,[6] Schwarzschild,[7] or Sutter[8] who obtained upper limits for $N_{\gamma\gamma}/N$ for this transition of 6×10^{-4}, 5×10^{-4}, and 6.4×10^{-4} respectively. Thus far no one has reported a positive effect in competition with the 3.35-MeV $E0$ transition in Ca^{40}. Sutter[8] obtained an upper limit of $N_{\gamma\gamma}/N\leq 2.1\times 10^{-3}$ for this transition.[8a]

Therefore, at the beginning of this experiment it appeared that the only case in which a positive double gamma-ray effect had been observed and not refuted was in competition with the 6.05-MeV $E0$ transition in O^{16}. In that case Sutter *et al.*[8] populated this state by the $F^{19}(p,\alpha)O^{16}$ reaction at the well known $E_p=1.88$-MeV resonance. The spectrum of alpha particles entering a junction counter at 150° to the beam was displayed on a pulse-height analyzer in triple coincidence with two 4-in.×4-in. NaI gamma-ray detectors, each channeled on the region from 1.5 to 4.5 MeV. An 8-cm-thick double-conical lead absorber separated the two NaI crystals. At the position of the unresolved $\alpha_{6.05}$ and $\alpha_{6.13}$ lines a net yield of 40 counts was obtained in an 80-h run, and this yield was attributed to double gamma-ray emission from the 6.05-MeV state. From their measurement Sutter *et al.*[8] calculated the ratio $\Gamma_{E1E1}/\Gamma_{E0(\pi)}=(2.5\pm 1.1)\times 10^{-3}$ for the 6.05-MeV state in O^{16}.

In two-photon transitions the sum of the energies of the two gamma rays involved, $E_\gamma(1)$ and $E_\gamma(2)$, must always equal the total transition energy E_0. Therefore in a two-dimensional plot of $E_\gamma(1)\times E_\gamma(2)$ transitions in which one of the photons loses all of its energy to one of the detectors and the other photon loses all of its energy to another detector should produce a line corresponding to $E_\gamma(1)+E_\gamma(2)=E_0$. Similar lines can be constructed for events in which not all of the gamma-ray energy is left in the detector, e.g., Compton events and pair events in which either one or both of the annihilation quanta escape from the detector. A study of the patterns in such an $E_\gamma(1)\times E_\gamma(2)$ array would allow one to discriminate against other real γ-γ coincidences such as γ-γ cascades and crosstalk between the detectors involving gamma rays with energies different

† Work performed under the auspices of the U. S. Atomic Energy Commission.

[1] G. J. McCallum, D. A. Bromley, and J. A. Kuehner, Nucl. Phys. **20**, 382 (1960).

[2] T. Alväger and H. Ryde, Phys. Rev. Letters **4**, 363 (1960) and Arkiv Fysik **17**, 535 (1960).

[3] R. E. Bell and R. L. Graham, Phys. Rev. **86**, 212 (1952).

[4] *Nuclear Data Sheets*, compiled by K. Way *et al.* (Printing and Publishing Office, National Academy of Sciences—National Research Council, Washington, 1961), NRC-61-2-48 ff.

[5] H. Langhoff and H. H. Hennies, Z. Physik **164**, 166 (1961).

[6] H. Ryde, Arkiv Fysik **23**, 247 (1963).

[7] A. Schwarzschild (private communication).

[8] G. Sutter, Ann. Phys. (Paris) **8**, 323 (1963); S. Gorodetzky, G. Sutter, R. Armbruster, P. Chevallier, P. Menrath *et al.*, Phys. Rev. Letters **7**, 170 (1961).

[8a] *Note added in proof*. P. Harihar and C. S. Wu [Bull. Am. Phys. Soc. **9**, 457 (1964)] have recently reported limits of $N_{\gamma\gamma}/N\leq 4\times 10^{-4}$ for the 3.35-MeV transition in Ca^{40} and $N_{\gamma\gamma}/N\leq(1.8\pm 1.0)\times 10^{-4}$ for the 1.75-MeV transition in Zr^{90}.

from that of the transition being studied. Hence, with a two-dimensional pulse-height analyzer, it was felt that by making a direct measurement of the intensity versus energy distribution of the coincident gamma-ray map more conclusive investigations of double gamma-ray emission could be carried out, not only in terms of searching for examples of this decay but also in terms of studying the energy spectrum of two-photon emission. In all the examples cited above involving double-$E1$ transitions this spectrum was assumed to have the theoretically predicted[9] form, $E^3(E_0-E)^3$, where E is the energy of one of the two gamma rays and E_0 is the total transition energy. On the basis of the positive result previously reported[8] for O^{16}, the yield of two-photon decays in the present experiment would have been quite sufficient for a study of the energy spectrum of that decay as a check on the theoretical prediction of $E^3(E_0-E)^3$. Hence, the present work was undertaken in order to look for this expected characteristic in the decay of the 6.05-MeV level of O^{16} and to make a search for double gamma-ray emission from the 4.43-MeV level of C^{12} that might be more sensitive than the previous investigation of McCallum *et al.*[1]

EXPERIMENTAL PROCEDURES AND RESULTS

A. The 6.05-MeV Level of O^{16}

In order to study the decay of the 6.05-MeV first excited state of O^{16}, this level was populated via the resonance in the $F^{19}(p,\alpha)O^{16}$ reaction at $E_p=1.88$ MeV using a target consisting of a 0.4 mg/cm^2 thick layer of CaF_2 evaporated on a 0.5 mg/cm^2 thick carbon foil backed with 0.020-in.-thick tantalum. This target was viewed by two 5-in.$\times$5-in. NaI detectors placed at 90° to the incident beam and 180° to each other. RCA-6342A 2-in.-diam photomultiplier tubes were mounted on the NaI scintillators to allow the use of fast coincidence techniques to reduce the background due to random coincidences. The outputs of E280F limiters, operating on signals derived from the anodes of the photomultiplier tubes, were used to drive a fast coincidence circuit with a resolving time of $\tau=12\times10^{-9}$ sec. Satisfactory operation of the coincidence circuit limiters was achieved for all pulses corresponding to energies above 0.7 MeV. The linear outputs of the detectors were amplified and fed, in triple coincidence with the output of the fast coincidence circuit, to a Chase-type 64$\times$64 channel two-dimensional pulse-height analyzer.[10] Timing adjustments, coincidence efficiency measurements and two-dimensional display tests were made with a Co^{60} source prior to each run.

Excitation curves for the production of pairs and for the production of high-energy gamma rays were measured in order to locate the resonances at $E_p=1.375$ MeV and $E_p=1.88$ MeV. At the lower resonance the 6.13-MeV gamma rays dominate the NaI spectrum, while at $E_p=1.88$ MeV the gamma rays of 6.9 and 7.1 MeV are considerably more abundant than the 6.13-MeV radiation. The population of the 6.05-MeV level relative to the sum of the populations of the gamma-emitting levels was found to be higher at the 1.88-MeV resonance by about a factor of 4 compared to the 1.375-MeV resonance, making the 1.88-MeV resonance the more favorable one to use in the present experiment.

In the initial runs the distance from the target to the front surface of each crystal was 5 cm, this being sufficient so that the energy of gamma rays Compton scattered in one crystal and able to reach the other crystal was less than 0.5 MeV. Enough absorber ($\frac{1}{8}$-in. of copper) was used in front of each crystal to remove the 6.05-MeV positron-electron pairs. In this geometry, two-dimensional coincidence runs that were made both at the 1.375-MeV and at the 1.88-MeV resonances exhibited surprisingly large numbers of real coincidences in a continuous distribution bounded by a line of constant total energy. Figure 1 shows a photograph of the data taken at the $E_p=1.88$-MeV resonance. The diagonal boundary line corresponds to a total energy of about $[E_\gamma(1)+E_\gamma(2)]=7$ MeV; in addition to the sharp boundary line a small yield of 7-MeV$\times$7-MeV random coincidences can be seen in the upper right-hand corner. For the data taken at the 1.375-MeV resonance the pattern was very similar to that in Fig. 1, except that the boundary line corresponded to a total energy of about 6 MeV.

For the case of double gamma-ray emission from the 6.05-MeV level in O^{16}, one would expect a pattern of real coincidences along the line corresponding to $[E_\gamma(1)+E_\gamma(2)]=6.05$ MeV, and the intensity profile along this line should have a maximum at its center. The spectrum and profiles in Fig. 1 indicate that the observed coincidence structure was characterized by an energy corresponding to that of the predominate gamma radiation (7 MeV in this case, 6 MeV at the 1.375-MeV resonance), and that the intensity profile along the line corresponding to a total energy, $[E_\gamma(1)+E_\gamma(2)]$, of 6.05 MeV has a deep minimum at its center. From this we conclude that in this geometry a major part of the real coincidences cannot be associated with the two-photon decay of the 6.05-MeV level of O^{16}.

As an explanation for the observed coincidence distribution, the following process may be considered: A high-energy gamma ray from the target produces a positron-electron pair in one of the crystals; the positron decays by annihilation in flight; the electron and the low-energy annihilation quantum stop in the first crystal; the high-energy annihilation quantum escapes and is detected in the second crystal, producing a real coincidence with a total energy equal to that of the original gamma ray. From Heitler's treatment of

[9] R. G. Sachs, Phys. Rev. **57**, 194 (1940).
[10] R. L. Chase, IRE Natl. Conv. Record **9**, 196 (1959).

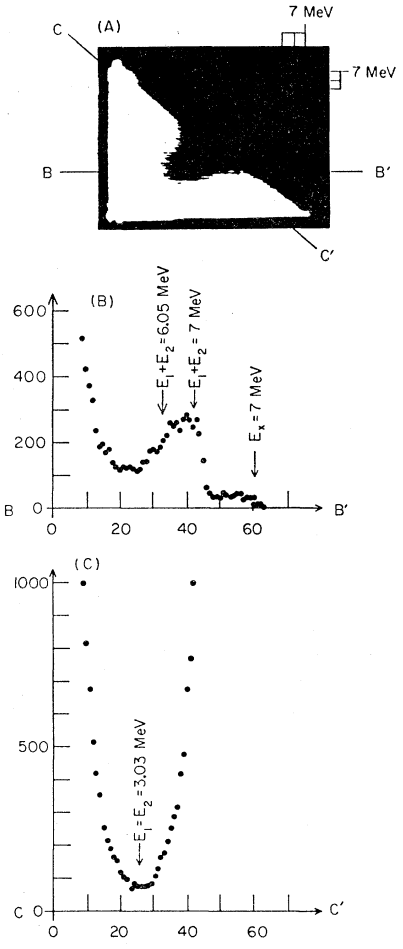

FIG. 1. Gamma-gamma coincidence data measured with two 5-in.×5-in. NaI scintillators at 90° to the incident beam and at 180° to each other without the use of extensive shielding between the detectors, for a 555-μC run at the $E_p=1.88$-MeV resonance in the $F^{19}(p,\alpha)O^{16}$ reaction. (A): Photograph of the 64×64 two-dimensional map display of the γ-γ coincidence pattern. In this, and in all other photographs of the map display in this paper, the energies of the two gamma rays are plotted along the X and Y axes, zero energy being in the lower left-hand corner. The bright areas correspond to channels in which the number of stored counts is above the particular contour level. In this particular photograph the counts in the upper right-hand corner correspond to 7-MeV ×7-MeV random coincidences. The lines BB′ and CC′ indicate the locations of the sections plotted below in parts (B) and (C) of this figure. (B): Section along the line BB′ above; this corresponds to $Y=15$ or $E_\gamma(y)=2.05$ MeV. The arrows indicate the locations where $E_\gamma(1)+E_\gamma(2)=6.05$ and 7 MeV, demonstrating that the principle structure in this section is associated with the high-energy gamma rays and not with the decay of the 6.05-MeV level. The relative contribution of random coincidences to this yield is indicated by the structure in this plot which extends beyond the point where $E_\gamma(1)+E_\gamma(2)=7$ MeV out to $E_\gamma(x)=7$ MeV. (C): Section along the line CC′ above; this corresponds to $E_\gamma(1)+E_\gamma(2)=6.05$ MeV. The arrow indicates the location of the center of the distribution, $E_\gamma(1)=E_\gamma(2)=3$ MeV, where a peak of the form $E^3(E_0-E)^3$ is predicted for double-$E1$ emission.

annihilation in flight[11] it is clear that the probability of annihilation in flight rises rapidly as the positron's energy decreases. The fact that this increase in the probability of annihilation in flight is faster than a linear relationship and the fact that we have two nearly identical detectors combine to predict from symmetry considerations that the intensity along the diagonal of an annihilation-in-flight coincidence pattern should have a minimum at its center, in qualitative agreement with the observed profile in Fig. 1. For positrons of several MeV the total probability for annihilation in flight is a few percent, and thus one should expect an appreciable amount of cross talk between crystals due to this effect if no bulk shielding is used. Even with bulk shielding, when the two crystals are on opposite sides of the target it will not be possible to completely eliminate this effect, and in an experiment of this nature with an extremely low counting rate this type of cross talk event may well still make a significant contribution to the coincidence yield.

In view of the above observations, the experimental arrangement shown in Fig. 2 was adopted. The bulk of the arrangement consists of a double-conical absorber with a half-angle of 38.7° and a total length of 16 cm. Most of the absorber is made of lead except for a central core (1.5 in. in diam) made of Hevimet (density of 17 g/cm^3). From a rough numerical integration it was calculated that for annihilation-in-flight quanta of about 3 MeV this double-conical absorber should reduce the cross-talk coincidences by a factor of about 12 as compared to the same geometrical configuration of detectors without absorber. The target, which is situated at the common apex of the two conical openings, is attached to the end of a $\frac{3}{8}$-in.-o.d. target tube introduced through a hole in the side of the absorber. At a distance of 7 in. in front of the target there is a tantalum aperture which collimates the beam to a 2-mm diameter at the target. A layer of Teflon tape insulates the target tube from the absorber in order that the beam current can be measured. For the O^{16} experiments, $\frac{1}{8}$-in.-thick copper absorbers were placed in the conical openings to keep the 6.05-MeV positron-electron pairs from interacting with the crystals. To obtain a reasonable real-to-random ratio, runs were made at a beam current of 0.03 μA.

The final data consisted of a 42-h real-coincidence run (4500 μC) and a 21-h random-coincidence run (2250 μC). Figure 3 shows a photograph of the data taken in the 42-h run and a photograph of the data taken during the 21-h random run and multiplied by a factor of 2 to match the 42-h run. Compared to the data in Fig. 1, note the large reduction in cross-talk coincidences relative to random coincidences although all three of these runs were made at essentially the same singles rate. Figure 3(A) and 3(B) are quite similar and match extremely well in the region of the 7-MeV×7-MeV yield in the upper right-hand corner which is caused entirely by randoms. However, since the estimated reduction in cross talk effected by the

[11] W. Heitler, *The Quantum Theory of Radiation* (Oxford University Press, New York, 1954), p. 384 ff.

absorber cannot be in error by more than a factor of 2 or 3, a continuum of real coincidences due to cross talk between the crystals must still be present in Fig. 3(A), even when the absorber is used. This continuum is visible in the lower left-hand quarter of Fig. 3(A). The subtraction of the properly normalized random-coincidence run further reveals that this real-coincidence continuum still extends to a sum-energy boundary of 7.0 ± 0.2 MeV, as seen in the profiles plotted in Figs. 3(C) and 3(D).

The arrow in Fig. 3(D) indicates the expected position in this spectrum of a peak due to the two-photon decay of the 6.05-MeV level of O^{16}. From an analysis of 18 such plots, 9 along the X axis and 9 along the Y axis, covering the central region around the 3-MeV $\times$3-MeV location of the peak in the $E^3(E_0-E)^3$ distribution, it can be concluded that in this grid of 81 channels there is no evidence for any consistent structure with a peak height greater than 10 counts per channel for the entire 42-h run.

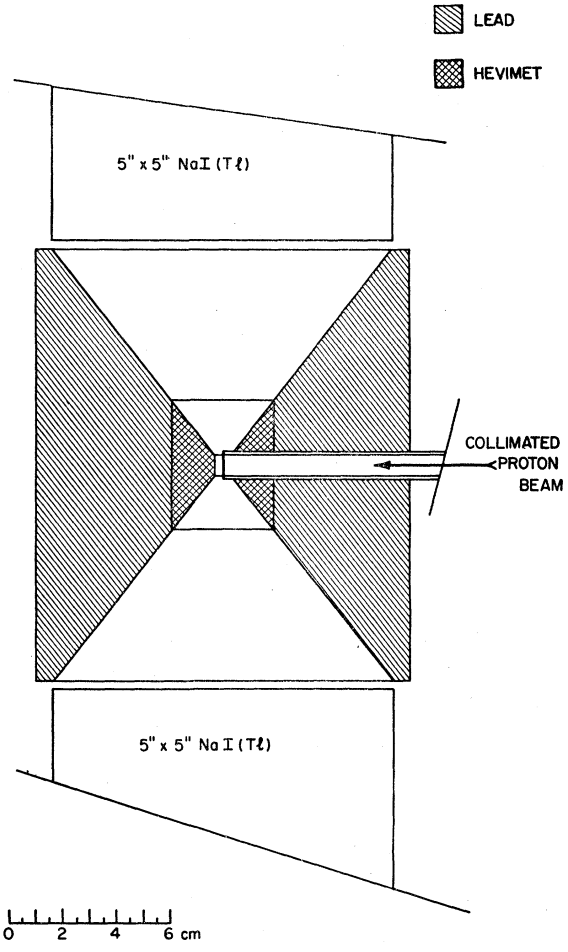

FIG. 2. Scale drawing of the target-detector geometry using the 16-cm double-conical lead-Hevimet shield. The shield is a solid cylinder from which two coaxial cones have been removed. The beam tube is admitted through a $\frac{3}{8}$-in. hole in the side of the cylindrical shield so that the target is at the apex of both cones.

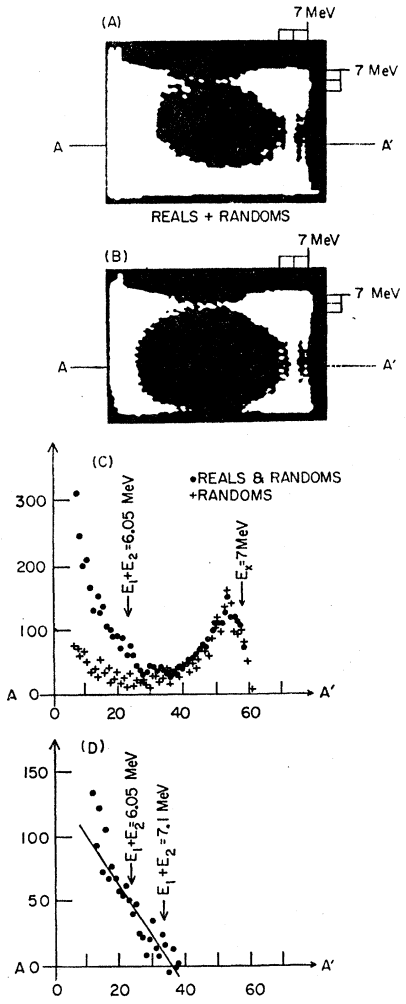

FIG. 3. Gamma-gamma coincidence data measured using the target-detector-shielding configuration shown in Fig. 2 for runs at the 1.88-MeV resonance in the $F^{19}(p,\alpha)O^{16}$ reaction. (A): Photograph of the 64$\times$64 two-dimensional map display [see Fig. 1(A)] of the 42-h 4500-μC real-coincidence run. (B): Photograph of the 64$\times$64 two-dimensional map display of the 21-h 2250-μC random-coincidence run, indicating the 7-MeV$\times$7-MeV random coincidence pattern. [The contour level here has been set only half as high as in (A) so that the two maps can be compared directly.] A comparison of (A) and (B) indicates that while most of the "real" run is due to random coincidences, there is a region of real coincidences in the lower left-hand quarter of (A). (C): Sections AA' of the map displays in Fig. 3(A) and (B); these correspond to $Y=23$ or $E_\gamma(y)=3.03$ MeV. (D): The net, real coincidences on section AA' above. The arrows indicate the expected position of a peak in the $E^3(E_0-E)^3$ double-$E1$ distribution at $E_\gamma(y)=E_\gamma(x)=3.03$ MeV and the endpoint of the observed distribution of real coincidences at $E_\gamma(1)+E_\gamma(2)\approx7$ MeV, corresponding to the high-energy gamma rays associated with the $F^{19}(p,\alpha)O^{16}$ reaction to the 6.9- and 7.1-MeV states in O^{16}.

Having obtained this upper limit on the number of double-gamma events possible at the peak of the $E^3(E_0-E)^3$ distribution, in order to compute the ratio $\Gamma_{E1E1}/\Gamma_{E0(\pi)}$ it is necessary to know the number of

6.05-MeV states populated per μC of integrated beam at the 1.88-MeV resonance. To measure this population the lead-Hevimet absorber over the end of the target tube was replaced by a lead cap with a wall thickness of about 3 mm, sufficient to stop all positrons except for the very small fraction that went back at 180° to the incident beam. The spectrum in the region of the 511-keV annihilation line was then recorded from one of the crystals on a 400-channel pulse-height analyzer for a charge accumulation of 0.25 μC. To find the total number of 6.05-MeV states formed per μC the photopeak area of the annihilation line was corrected for analyzer deadtime, absorber thickness, total efficiency, peak-to-total ratio and the factor of 2 for the number of annihilation quanta per transition. The distribution of annihilation quanta was taken to be isotropic. The result was 1.80×10^6 6.05-MeV states formed per μC (54 000 per second at 0.03 μA) and a total of 8.10×10^9 for the 42-h run.

B. The 4.43-MeV Level of C^{12}

For the investigation of double gamma-ray emission from the 4.43-MeV level of C^{12} the reaction $N^{15}(p,\alpha)C^{12}$ was used to populate the state. The experimental arrangement (see Fig. 2) was similar to that used in the O^{16} experiment except that the $\frac{1}{8}$-in.-thick copper absorbers used in the O^{16} work to stop the 6.05-MeV positron-electron pairs were removed. The target was a 12-mg/cm^2-thick zirconium foil that had been nitrided in an atmosphere of nitrogen gas enriched to 96% N^{15}, resulting in a surface layer of ZrN^{15} with approximately 15 μg/cm^2 of N^{15}. Resonances in the $N^{15}(p,\alpha)C^{12}$ reaction populating the 4.43-MeV state were located by measuring the yield of 4.43-MeV gamma rays as a function of the beam energy.

McCallum *et al.*[1] had observed the presence of interfering coincident gamma rays from the $N^{15}(p,\gamma)O^{16}$ reaction at the $E_p=0.898$-MeV resonance. Their observations are confirmed in the data which we have obtained at that resonance, shown in Fig. 4. In these two photographs, taken at different contour levels of the 64×64 map display for the same run, the various lines and peaks in addition to the 4.43-MeV×4.43-MeV random structure can all be identified with cascades in the O^{16} nucleus resulting from the $N^{15}(p,\gamma)O^{16}$ reaction through the 12.97-MeV excited state of O^{16}. These cascades include the 6.84-MeV+6.13-MeV transition through the 6.13-MeV level and the 4.09-MeV transition to the 8.88-MeV level together with all the cascades from the 8.88-MeV level, the strongest of which is the 2.75-MeV+6.13-MeV cascade through the 6.13-MeV level.

Runs made at the $E_p=1.21$-MeV resonance confirm the conclusion of McCallum *et al.*[1] that this resonance is more favorable than the 0.898-MeV resonance for a search for the two-photon decay of the 4.43-MeV level of C^{12} because of the relatively smaller number of (p,γ) capture gamma rays. In fact, in none of the data taken at the 1.21-MeV resonance could any evidence be seen

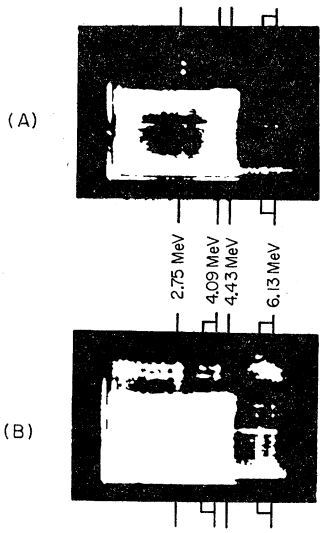

FIG. 4. Gamma-gamma coincidence data measured using the target-detector-shielding configuration shown in Fig. 2, for a run of 21 000 μC at the 898-keV resonance in the $N^{15}(p,\alpha)C^{12}$ reaction. (A): Photograph of the 64×64 two-dimensional map display [see Fig. 1(A)] showing the 4.43-MeV×4.43-MeV random-coincidence pattern as well as the pattern of real coincidences from the 4.09-MeV+2.75-MeV+6.13-MeV cascade from the 12.97-MeV state in O^{16} via the reaction $N^{15}(p,\gamma)O^{16}$. (B): Photograph of the same data shown in Fig. 4(A) but taken at a lower contour level, showing in addition to the patterns noted in Fig. 4(A) the 6.84-MeV+6.13-MeV cascade from the 12.97-MeV state in O^{16}.

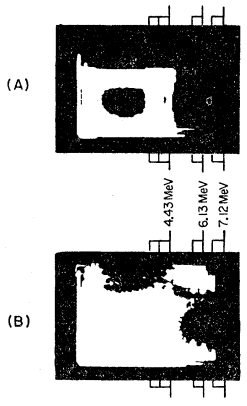

FIG. 5. Gamma-gamma coincidence data measured using the target-detector-shielding configuration shown in Fig. 2, for a run of 54 000 μC at the 1.21-MeV resonance in the $N^{15}(p,\alpha)C^{12}$ reaction. (A): Photograph of the 64×64 two-dimensional map display [see Fig. 1(A)]. The run shown here and that shown in Fig. 4 were taken at essentially the same singles rates. Note the complete absence of any pattern of real coincidences from γ-γ cascades, especially in the central region of the map. (B): Photograph of the same data shown in Fig. 5(A) but taken at a much lower contour level, showing evidence for a weak 7.12-MeV+6.13-MeV cascade from the 13.25-MeV state in O^{16} via the $N^{15}(p,\gamma)O^{16}$ reaction. Note, however, the complete absence of any evidence for any other cascades involving lower energy gamma rays such as are seen in Fig. 4.

for cascade transitions through the 8.88-MeV level of O^{16}. Figure 5 shows photographs of data taken at the 1.21-MeV resonance for a total charge accumulation of 54 000 μC revealing the presence of cascade transitions from the 13.25-MeV state in O^{16} only through the 7.12-MeV state and/or the 6.13-MeV state. However, the region of interest around the peak in the $E^3(E_0-E)^3$ distribution at 2.2-MeV$\times$2.2-MeV appears very clean in the sense of freedom from low-energy cascade radiations, specifically the gamma rays associated with the decay of the 8.88-MeV level.

In order to obtain a reasonable real-to-random ratio, final data for the 4.43-MeV C^{12} level were taken at a beam current of 0.30 μA. At this current a 43-h run (50 000 μC) was made at the 1.21-MeV resonance, followed by a 24-h (26 500 μC) random run at the same resonance under identical conditions. After proper normalization the random run was subtracted from the 43-h run to obtain the net real coincidences. These net results for the C^{12} case are similar to those found for O^{16}, i.e., a broad continuum of coincidences extending to an end point corresponding to $[E_\gamma(1)+E_\gamma(2)]\sim 4.5$ MeV. The number of real counts contributed to this distribution by the cascade transitions, $13.25\rightarrow 7.12\rightarrow 0$ and/or $13.25\rightarrow 6.13\rightarrow 0$, was calculated on the basis of the shapes of these gamma rays as observed in the $F^{19}(p,\alpha)O^{16}$ reaction. This contribution turned out to be only a small fraction of the continuum effects associated with annihilation in flight from the 4.43-MeV gamma rays. A profile along the line corresponding to a total energy of 4.43 MeV exhibits a minimum at its center, and a search of the region around the predicted location of the peak in the $E^3(E_0-E)^3$ distribution, in the same manner as in the O^{16} case, reveals no consistent structure with a peak height greater than 20 counts per channel for the entire 43-h run.

To measure the population of the 4.43-MeV level, the singles spectrum from one of the NaI scintillators was recorded on a 400-channel pulse-height analyzer. These data were then treated in the conventional manner described previously for the O^{16} experiment, taking into account the observed[12] anisotropy of the 4.43-MeV gamma rays from this resonance,

$$W(\theta)=P_0(\cos\theta)+(0.45\pm 0.01)P_2(\cos\theta) - (0.30\pm 0.01)P_4(\cos\theta),$$

where θ is the angle between the gamma ray and the direction of the incident beam. This gave the rate of production of the 4.43-MeV state as 5.48×10^5 per μC (1.65×10^5 per sec at 0.3 μA) and a total of 2.74×10^{10} for the 43-h run.

ANALYSIS AND DISCUSSION

In this section we will combine the limits derived above for the number of observed two-photon decays and the measured populations of the decaying levels to obtain limits for the branching ratios, $\Gamma_{E1E1}/\Gamma_{E0(\pi)}$ and $\Gamma_{E1E1}/\Gamma_{E2}$ for the 6.05-MeV level in O^{16} and the 4.43-MeV level in C^{12}, respectively. The theoretically predicted[9] energy spectrum of the gamma rays produced in the double-$E1$ decay is of the form

$$f(E)\propto E^3(E_0-E)^3 \equiv AE^3(E_0-E)^3$$

and has a maximum at $E=E_0/2$. The total number of double-gamma decays is given by $F(E_0)$, the integral over $f(E)$,

$$F(E_0)=\int_0^{E_0} f(E)dE = (A/140)E_0^7 = (64/140)E_0 f(E_0/2),$$

where $f(E_0/2)$ is the height of the distribution at its maximum. In our experiment we have attempted to determine a value for $F(E_0)$ by measuring $f(E_0/2)$. Defining C as the limits we have derived in the preceding section for the number of observed two-photon decays (the maximum peak height of any consistent structure in the neighborhood of the $E_0/2\times E_0/2$ peak in the $E^3(E_0-E)^3$ distribution), $f(E_0/2)$ can be expressed as

$$f(E_0/2)=C\left(\frac{\Delta Ch}{\Delta E}\right)\frac{1}{\mathrm{EFF}},$$

where $(\Delta Ch/\Delta E)$ defines the dispersion of our spectra (typically $\sim$9 channels/MeV) and EFF is the efficiency for detecting an $E_\gamma(1)=E_\gamma(2)=E_0/2$ event exactly in the $E_0/2\times E_0/2$ channel. In addition, to just the efficiency for detecting gamma rays of energy $E_0/2$ in this geometry, such a term must also include such effects as the angular distributions and angular correlations of these gamma rays, the absorption by materials between the target and the crystals, the peak-to-total ratios of the detectors, and the resolution of the detectors, since the width of the full-energy peaks of these gamma rays is large compared to the one channel we are considering. Using the standard tabulations of Sharp *et al.*[13] we have obtained the following pertinent angular distributions and angular correlations:

(1) For the O^{16} case we consider the two-photon decay to be described by

$$0^+ \xrightarrow{\gamma_1(E1)} 1^- \xrightarrow{\gamma_2(E1)} 0^+$$

and take the angular distribution of γ_1 with respect to the beam to be isotropic and the angular correlation

[12] S. Bashkin and R. R. Carlson, Phys. Rev. **106**, 261 (1957).

[13] W. T. Sharp, J. M. Kennedy, B. J. Sears, and M. G. Hoyle, Chalk River Report, CRT-556, 1954 (unpublished).

between γ_1 and γ_2 to be given by

$$W_{12}(\theta_{12})=P_0(\cos\theta_{12})+0.50P_2(\cos\theta_{12}).$$

(2) For the C^{12} case we consider the two-photon decay to be described by

$$2^+ \xrightarrow{\gamma_1(E1)} 1^- \xrightarrow{\gamma_2(E1)} 0^+$$

and take the angular distribution of γ_1 with respect to the beam to be given by

$$W_1(\theta_1)=P_0(\cos\theta_1)-0.343P_2(\cos\theta_1)$$

and the angular correlation between γ_1 and γ_2 to be given by

$$W_{12}(\theta_{12})=P_0(\cos\theta_{12})-0.250P_2(\cos\theta_{12}).$$

Using these angular correlations, the total efficiency for detecting a $\gamma_1\times\gamma_2$ coincidence was calculated as

$$\eta_0(\gamma_1,\gamma_2)=\left[\int_0^{2\pi}d\phi\int_0^{\pi}W_1(\theta)\sin\theta d\theta \times\int_0^{2\pi}d\phi\int_0^{\pi}W_{12}(\theta)\sin\theta d\theta\right]^{-1} \times\left\{\int_A W_1(\theta_1)(1-e^{-\tau_1 X(\theta_A)})d\Omega_A \times\int_B W_{12}(\theta_{12})(1-e^{-\tau_2 X(\theta_B)})d\Omega_B +\int_B W_1(\theta_1)(1-e^{-\tau_1 X(\theta_B)})d\Omega_B \times\int_A W_{12}(\theta_{12})(1-e^{-\tau_2 X(\theta_A)})d\Omega_A\right\},$$

where A and B denote the two NaI crystals involved and where for the purpose of calculation $W_1(\theta_1)$ and $W_{12}(\theta_{12})$ must be re-expressed in terms of θ_A and θ_B by making use of the addition theorem (e.g., Rose[14]).

The resolutions of the two detectors in a two-dimensional plot can be transformed along the X and Y axes to resolutions parallel and perpendicular to a line of constant total energy. In this configuration it is clear that the resolution parallel to the line of constant total energy will not effect our result since to first order as much yield will be spilled into our peak channel from other events along this line as will be spilled out. The resolution perpendicular to the line of constant total energy will, however, decrease our efficiency. In our present measurements it turned out that the dispersion and the resolution of the crystals at $E_\gamma=E_0/2$ were such that the full width at half-maximum was very nearly 2.0 channels for both the O^{16} and the C^{12} cases. Thus, the resolution perpendicular to the line of constant total energy will reduce the efficiency by a factor of 2.

Combining all these effects with the measured peak-to-total ratios, ϕ_0, and the absorption, ABS, of the materials between the target and the crystals, we calculate EFF as

$$\text{EFF}=\eta_0(\gamma_1,\gamma_2)\times(\tfrac{1}{2})\times\phi_0(\gamma_1)\times\phi_0(\gamma_2)\times\text{ABS}(\gamma_1)\times\text{ABS}(\gamma_2).$$

In the geometry shown in Fig. 2 a calculation of EFF yields 2.74×10^{-4} for the O^{16} experiment and 2.86×10^{-4} for the C^{12} experiment.

Combining these values of EFF with the appropriate values for C, $(\Delta Ch/\Delta E)$, and E_0, we have the following limits for $F(E_0)$:

$$F(E_0)_{\text{42-h run on O}^{16}}\leq0.885\times10^6,$$
$$F(E_0)_{\text{43-h run on C}^{12}}\leq1.31\times10^6.$$

These limits on the total number of two-photon decays, together with the populations measured above, yield

$$(\Gamma_{E1E1}/\Gamma_{E0(\pi)})_{\text{6.05-MeV level in O}^{16}}\leq1.1\times10^{-4}$$
$$(\Gamma_{E1E1}/\Gamma_{E2})_{\text{4.43-MeV level in C}^{12}}\leq0.5\times10^{-4}.$$

This limit on the double-gamma emission of the 4.43-MeV level in C^{12} is a factor of 3 lower than the limit of 1.7×10^{-4} obtained by McCallum *et al.*[1] but is still considerably larger than the value of 10^{-8} predicted for this transition by Lane and Soper.[15] The limit derived above for the decay of the 6.05-MeV level in O^{16} by double gamma emission is approximately a factor of 20 lower than the value of $(2.5\pm1.1)\times10^{-3}$ measured by the Strasbourg group.[8] This discrepancy can probably be understood in terms of cross talk between the two NaI crystals associated with the annihilation in flight of positrons produced by high-energy gamma rays, as described above. This effect was not taken into account in the work of the Strasbourg group, and their double-conical lead shielding was not as effective in reducing this effect as the shielding configuration we have used. Indeed the magnitude of the effect one would expect from annihilation in flight using the Strasbourg shielding is such that one can qualitatively account for their measurement in terms of events of the type $[\alpha_{6.13}-\gamma\gamma$ (6.13-MeV annihilation in flight)].

In conclusion, in view of all the measurements reported up to the present time it appears that the decay of excited nuclear levels by the second-order interaction of double gamma emission has thus far not been observed.

[14] M. E. Rose, Phys. Rev. **91**, 610 (1953).

[15] A. M. Lane and J. M. Soper (private communication as quoted in Ref. 1).